agriculture

MDPI

Article

Identification of the Citrus Superoxide Dismutase Family and Their Roles in Response to Phytohormones and Citrus Bacterial Canker

Wen Yang [1], Jia Fu [1], Xin Huang [1], Jie Fan [1], Xiujuan Qin [1], Qiyuan Yu [1], Chenxi Zhang [1], Baohang Xian [1], Shanchun Chen [1,2,3], Yongrui He [1,2,3] and Qiang Li [1,2,3,*]

[1] Citrus Research Institute, Southwest University, Chinese Academy of Agricultural Sciences, Chongqing 400712, China
[2] National Citrus Engineering Research Center, Chongqing 400712, China
[3] National Citrus Improvement Center, Chongqing 400712, China
* Correspondence: liqiang@cric.cn; Tel.: +86-(0)-23-68349019

Abstract: Superoxide dismutases (SODs) play critical roles in plants, especially in the maintenance of redox homeostasis. The response of SODs in Citrus (*Citrus sinensis* (L.) Osbeck) to citrus bacterial canker (CBC) infection were investigated. The CsSODs were identified, and their gene structures, phylogeny, conserved domains and motifs, predicted interactions, and chromosomal distribution were analyzed. CsSOD expression in response to stress-related plant hormones (salicylic acid, SA; methyl jasmonate, MeJA; and abscisic acid, ABA) and *Xanthomonas citri* subsp. *citri* (*Xcc*) infection were also investigated. Thirteen CsSODs were identified in *C. sinensis*, including four Fe/MnSODs and nine Cu/ZnSODs with typical functional domains. The CsSODs were distributed on chromosomes 3, 5, 7, and 8. Specific hormone-response motifs were identified in the gene promoter regions. Ten genes were induced by MeJA treatment, as shown by qRT-PCR, and were upregulated in the CBC-susceptible Wanjincheng citrus variety, while *CsSOD06* and *CsSOD08* were upregulated by ABA in both the Wanjincheng and the CBC-resistant Kumquat varieties. *Xcc* infection significantly altered the levels of most CsSODs. The overexpression of *CsSOD06* and *CsSOD08* resulted in increased hydrogen peroxide levels and SOD activity. Our findings highlight the significance of SOD enzymes in the plant response to pathogen infection and have a potential application for breeding CBC-tolerant citrus varieties.

Keywords: citrus bacterial canker (CBC); superoxide dismutase (SOD); *Xanthomonas citri* subsp. *citri* (*Xcc*); salicylic acid (SA); jasmonic acid (JA)

check for updates

Citation: Yang, W.; Fu, J.; Huang, X.; Fan, J.; Qin, X.; Yu, Q.; Zhang, C.; Xian, B.; Chen, S.; He, Y.; et al. Identification of the Citrus Superoxide Dismutase Family and Their Roles in Response to Phytohormones and Citrus Bacterial Canker. *Agriculture* **2022**, *12*, 1254. https://doi.org/10.3390/agriculture12081254

Academic Editor: Gaetano Distefano

Received: 20 July 2022
Accepted: 16 August 2022
Published: 18 August 2022

1. Introduction

Plants are exposed to a variety of stresses, both biotic and abiotic, that may lead to metabolic disorders and even death [1]. Hydrogen peroxide (H_2O_2) is a relatively long-lived reactive oxygen species (ROS) that regulates many biological processes in plants, including growth, development, senescence, and death, as well as the plant's response to various stresses. Superoxide dismutases (SODs) are antioxidant enzymes that control ROS levels through the removal of excess free radicals, thus maintaining homeostasis and protecting the plant [2,3]. Specifically, SOD catalyzes the dismutation of superoxide anions into H_2O_2 and O_2 [4]. SOD was initially described in bovine erythrocytes [5]. Multiple *SOD* genes are usually present in plants and have been described in various plant species, including foxtail millet, Arabidopsis, tomato, and poplar, amongst many others [2]. Plant SODs are classified according to their metal cofactor and/or subcellular distribution and include copper–zinc SODs (Cu/ZnSOD) expressed in the cytoplasm, iron SODs (FeSOD), and manganese SODs (MnSOD) found in mitochondria [6]. Moreover, SOD enzymes within a species may differ both in terms of subcellular location and transcriptional regulation [7–9].

For instance, in Arabidopsis, SOD expression is closely related to thermotolerance [10] and growth under conditions of oxidative stress [11], and although they are both found in chloroplast thylakoids, *AtFSD2* and *AtFSD3* are not functionally interchangeable [12].

SOD enzymes have multiple functions in plants and are specifically associated with stress responses. For example, in transgenic rice plants, MnSOD from peas participates in the ROS-scavenging system of chloroplasts, leading to improved drought tolerance in rice [13]. Another study reported increased resistance to salt stress tolerance in Arabidopsis transgenic lines that overexpress superoxide dismutase [14]. Compared with the wild-type, the SOD activities and plant weights of MnSOD-transgenic plants were found to increase after exposure to NaCl stress [15]. *SOD* genes have also been associated with the plant response to stress-related phytohormones. Treatment with abscisic acid (ABA) upregulated the levels of a transcription factor associated with desiccation in *AtSOD*-transgenic plants, leading to the elimination of O_2 [16].

SODs function as a first line of defense in the plant immune response [7]. The enzymes have been found to enhance plant resistance to a variety of pathogens. Several SODs are involved in rice resistance to Magnaporthe oryzae fungus via upregulated H_2O_2 concentration [17], while *XcSOD*, an annotated gene from the *X. citri* subspecies, has been associated with the pathogenesis of citrus canker [18]. In addition, changes in SOD enzyme activity in plants can be used as biochemical markers for plant disease resistance and can play important roles in disease resistance mechanisms. SODs have been found to play important roles in plant resistance to bacterial diseases. For instance, plum pox virus (PPV) infection in the susceptible Real Fino apricot variety was observed to reduce SOD activity, in contrast with the elevated SOD activity seen in the resistant variety Stark Early Orange [19]. Mild symptoms were seen in conjunction with increased SOD activity after cotton infection with *Verticillium dahliae Kleb* [20], with *VdSOD5* found to be responsible for superoxide detoxification in the roots [21]. More importantly, there is specific evidence linking SOD overexpression in transgenic plum plants with resistance against bacterial canker [22]. A proteomic analysis of the response of tomato plants to a bacterial canker infection controlled by the locus showed the presence of three SOD enzymes, suggesting the involvement of these enzymes in resistance to *Clavibacter michiganensis* subsp. infection [23].

Citrus is a popular fruit crop throughout the world. In recent decades, its growth and yields have been threatened by citrus bacterial canker (CBC), caused by *Xanthomonas citri* subsp. *citri* (*Xcc*) [24,25]. As described above, SOD enzymes are known to regulate plant resistance to bacterial canker; however, these enzymes have not been well-studied in citrus. The identification of SOD enzymes and their functions would assist with the improvement of stress tolerance in citrus. Here, we used bioinformatics to analyze the *SOD* gene family and explore the expression of its members in response to *Xcc* infection and phytohormones (methyl jasmonate, MeJA; abscisic acid, ABA; and salicylic acid, SA). The findings extend our understanding of the associations between *SODs* and CBC infection and identify suitable genes for molecular breeding.

2. Materials and Methods

2.1. Plant and Bacterial Materials

The Wanjincheng (*C. sinensis*) and Kumquat (*C. japonica* Swingle) citrus cultivars were obtained from the National Citrus Germplasm Repository, Chongqing, China (19°51′ N, 106°37′ E). The plants were maintained in a greenhouse at 28 °C where they were used for CBC and exogenous hormone assays. The *Xcc* strain was obtained from the Citrus Research Institute of Southwest University.

2.2. Identification of SOD Genes in the Sweet Orange Genome

A three-step identification method was used for the identification of potential SOD genes in the citrus genome. Genomic and proteomic data were downloaded from the Citrus Pan-Genome to Breeding Database [26,27] (CPBD: http://citrus.hzau.edu.cn/, accessed on 1 October 2021) and Phytozome V12 (https://phytozome.jgi.doe.gov/pz/portal.html,

accessed on 2 October 2021) database, and a local database was constructed using Bioedit V7.0 (Creator:Thomas Hall, Los Angeles, CA, USA). SOD sequences from Arabidopsis were obtained from The Arabidopsis Information Resource (TAIR, https://www.arabidopsis.org, accessed on 1 October 2021) [28] and were used to query the local citrus protein database to obtain initial batches corresponding to the CsSOD family. A functional re-annotation of the sequences was performed using hidden Markov model (HMM) profiles downloaded from the Pfam2 database. The Simple Modular Architecture Research Tool (SMART: http://smart.embl.de/, accessed on 15 October 2021) was used to verify the integrity of the SOD domain in each CsSOD sequence. Redundant and putative protein sequences were excluded, and only sequences with verified conserved SOD domains were used for further analysis. In all, 13 citrus SODs were identified and used for further analysis. Information on the coding and promoter sequences, chromosomal location, and conserved domains were obtained from the CPBD.

2.3. In Silico Characterization of CsSODs

The predicted physicochemical properties of the CsSODs were analyzed by ExPASy (http://web.expasy.org/protparam/, accessed on 13 October 2021) [29]. Sequence alignment and maximum-likelihood phylogenetic tree compilation were performed using MEGA V7.0 (https://www.mega.com/, accessed on 13 October 2021) [30]. GSDS V2.0 (http://gsds.cbi.pku.edu.cn, accessed on 13 October 2021) [31] was used for gene structure visualization, and conserved motifs were identified with MEME V5.1 (http://memesuite.org/tools/meme, accessed on 12 October 2021) [32]. Chromosomal localization was analyzed with MAPCHART V2.1 [33], and CELLO (http://cello.life.nctu.edu.tw/, accessed on 12 October 2021) [34] was used to predict subcellular localizations. Protein secondary structures were predicted by PRABI (http://www.prabi.fr, accessed on 15 October 2021), and Pfam (http://pfam.xfam.org/, accessed on 12 October 2021) [35] was used for domain identification. Promoter cis-elements were predicted by PLANTCARE (http://bioinformatics.psb.ugent.be/webtools/plantcare/html/, accessed on 8 October 2021) [36]. Protein–protein interaction (PPI) networks were constructed by STRING V11.0 (https://cn.string-db.org/cgi/input?sessionId=bzp0URl1kGZD&input_page_show_search=on, accessed on 11 October 2021) [37], with an edge confidence > 0.4. TBTOOLS [38] was used to analyze promoter sequences and the syntenic relationships between CsSODs and AtSODs. Transcription factor binding sites in the promoters were predicted using JASPAR, with a relative profile score threshold of 98% (https://jaspar.genereg.net/, accessed on 13 October 2021) [39]. Heatmaps were drawn using Heatmapper (http://www.heatmapper.ca/expression/, accessed on 13 October 2021) [40].

2.4. Xcc and Phytohormone Treatments

Sample leaves from Wanjincheng and Kumquat were disinfected with 75% ethanol, washed three times with distilled water, and placed in culture plates. The leaves were then infected with *Xcc* dilutions (OD_{600}: 0.5) and incubated at 28 °C. Samples were taken at 0, 12, 24, 36, and 48 h after inoculation (hours post-inoculation; hpi), frozen in liquid nitrogen, and used for qRT-PCR determinations. Leaf discs (7 mm diameter) were immersed in MeJA (100 $\mu mol \cdot L^{-1}$), ABA (100 $\mu mol \cdot L^{-1}$), or SA (10 $\mu mol \cdot L^{-1}$) solutions or sterile water (control). Samples were taken at 0, 12, 24, 36, and 48 h post-treatment (hpt) and immediately frozen in liquid nitrogen before qRT-PCR analysis.

2.5. RNA Extraction and qRT-PCR Analysis

RNA was extracted from the samples using miniprep kits (AidLab, Beijing, China), following the provided protocols. TaKaRa kits (TaKaRa, Japan) were used to reverse-transcribe the RNA to cDNA. Specific primers for qRT-PCR analysis were designed using NCBI Primer BLAST according to CsActin (GenBank: GU911361.1), which was used as the internal control (Table S1). The qRT-PCR thermal cycle was as follows: 50 °C for 60 s, 95 °C pre-degeneration for 2 min, 40 cycles of 95 °C for 5 s and 60 °C for 15 s. A 12 µL reaction

mixture containing 100 ng of cDNA, 0.3 μM primer, and 6 μL of PCR mix was prepared. The expression of each gene was measured in triplicate from three biological replicates, and relative expression levels were calculated using the $2^{-\Delta\Delta Ct}$ (ΔCt = Ct CsSOD − Ct Actin) Ct method [41]. SPSS V22 was used to analyze differences using Duncan's LSD multiple range test ($p \leq 0.05$).

2.6. Transient Expression of CsSOD06 and CsSOD08 in Citrus

The expression vector pLGN, containing the *CsSOD06,08* CDS, was constructed and transformed into the *Agrobacterium tumefaciens* receptor EHA105. Leaves from the Wanjincheng variety were disinfected with 75% ethanol, washed three times with distilled water, and placed in culture plates. The Agrobacterium was injected into the citrus leaves, and the infected sites were sampled and assayed after incubation for five days at 28 °C.

2.7. Biochemical Indices

Hydrogen peroxide levels were determined as described by Velikova et al. (2000). Fresh leaves were homogenized in 2 mL of 0.1% trichloroacetic acid and centrifuged at 12,000× *g* for 15 min. Then, 500 μL of supernatant was added to the reaction mixture containing 0.5 mL of 10 mM K phosphate buffer (pH = 7.0) and 1 mL of 1 M KI. The blank controls did not contain samples. The H_2O_2 concentrations were determined from comparisons of OD390 values against a standard curve.

SOD activity was detected as follows: Fresh leaves were ground in 5 mL of 0.05 mol/L phosphate buffer (pH = 7.0) and centrifuged at 10,000× *g* for 20 min. Then, 100 μL of supernatant was added to the reaction mixture containing 3.1 mL of 0.05 mol/L phosphate buffer (pH = 7.8), 0.2 mL of 1 mg/mL EDTA-Na_2, 0.2 mL of 20 mg/mL L-methionine, 0.2 mL of 0.1 mg/mL riboflavin, and 0.2 mL of 1 mg/mL NBT. The blanks did not contain samples. Absorbances were measured at 390 nm, and SOD activity (U/g FW) was calculated as (ACK−AE) × 5/ACK × W × 0.2, where ACK is the first group of absorbance values, AE is the second group, and W is the weight of the fresh leaves.

2.8. Statistical Analysis

Data were analyzed using SPSS V22 (IBM Corp., Armonk, NY, USA). Gene expression was compared by an analysis of variance (ANOVA), and statistical significance was determined using Tukey's HSD test ($p = 0.05$).

3. Results

3.1. Genome-Wide Distribution of the Citrus SOD Gene Family

Thirteen CsSODs were identified in the *C. sinensis* genome. The physicochemical predictions showed that the molecular weights ranged between 14.151 and 37.913 kDa. The deduced protein sequences varied in length from 139 to 352 amino acids with aliphatic index values ranging from 67.29 to 93.81 and pIs between 4.63 and 9.42, with nine of the proteins being acidic. Significant differences in the instability index values of the CsSOD proteins were observed, ranging from 3.40 to 47.65, with most proteins predicted to be unstable, except for *CsSOD02* and *CsSOD07*. The grand average of hydropathicity (GRAVY) values varied between −0.674 and 0.150. Apart from *CsSOD02* and *CsSOD13*, all the SOD proteins were hydrophilic. The citrus SOD family proteins were mostly predicted to be located in the extracellular, cytoplasmic, chloroplast, and mitochondrial compartments. *CsSOD10* was predicted to be expressed in both the chloroplast and cytoplasm, while *CsSOD11* was predicted to be located in the chloroplast and mitochondria (Table 1).

Table 1. The CsSOD family.

Name	CAP ID	Size (aa)	Molecular Weight (Da)	Isoelectric Point (PI)	Grand Average of Hydropathicity	Aliphatic Index	Instability Index	Subcellular Localization
CsSOD01	Cs_ont_3g017650.1	352	37,912.86	6.92	−0.572	69.80	28.48	Extracellular
CsSOD02	Cs_ont_3g017660.1	139	14,150.98	6.24	0.150	93.81	10.49	Extracellular/ Cytoplasmic
CsSOD03	Cs_ont_3g017710.1	183	19,859.86	9.42	−0.163	88.42	22.20	Extracellular/ Cytoplasmic
CsSOD04	Cs_ont_3g017720.1	192	21,355.90	6.72	−0.320	79.64	26.48	Extracellular
CsSOD05	Cs_ont_3g017760.1	156	16,609.34	4.63	−0.251	79.36	18.03	Cytoplasmic
CsSOD06	Cs_ont_3g017770.1	156	16,150.05	5.50	−0.128	77.37	16.70	Cytoplasmic
CsSOD07	Cs_ont_5g014800.1	146	14,885.84	6.78	−0.112	90.82	3.40	Cytoplasmic
CsSOD08	Cs_ont_5g041000.1	248	26,520.07	7.76	−0.150	79.80	36.60	Chloroplast
CsSOD09	Cs_ont_7g013920.1	270	30,095.09	8.57	−0.439	74.52	36.92	Chloroplast
CsSOD10	Cs_ont_7g013930.1	303	34,616.86	5.22	−0.674	67.29	47.65	Cytoplasmic/ Chloroplast
CsSOD11	Cs_ont_7g019080.1	259	29,467.85	8.66	−0.275	85.83	31.53	Mitochondrial/ Chloroplast
CsSOD12	Cs_ont_7g002980.1	228	25,288.88	6.79	−0.212	92.81	36.56	Mitochondrial
CsSOD13	Cs_ont_8g006180.1	234	23,705.69	6.66	0.037	89.19	27.29	Chloroplast

All information on the SODs of C. sinensis was extracted from the Citrus Pan-Genome to Breeding Database (CPBD: http://citrus.hzau.edu.cn/, accessed on 13 October 2021). The physicochemical properties were analyzed by ExPASy, and subcellular loci were predicted by CELLO V2.5.

Secondary structure predictions indicated the presence of alpha helices, beta turns, random coils, and extended strands. *CsSOD01–07* and *CsSOD13* were predicted to consist largely of random coils and extended strands, while *CsSOD08–12* were mainly composed of alpha helices (Figure 1).

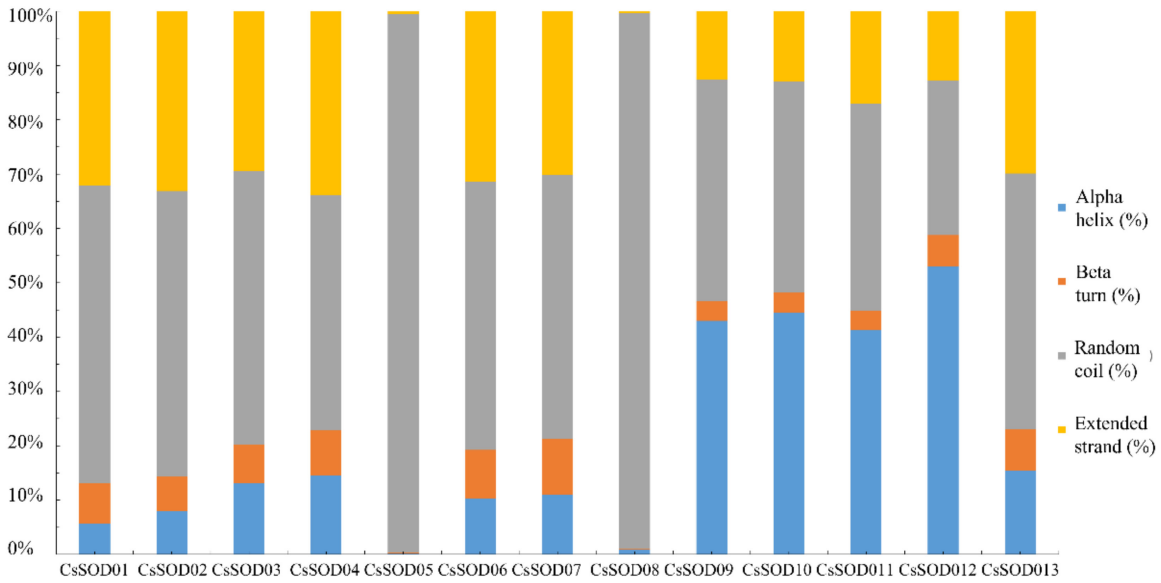

Figure 1. The secondary structures of CsSODs. The secondary structures were analyzed by PRABI.

3.2. Chromosomal Distribution and Intron/Exon Configurations of CsSOD Genes

The CsSOD genes were unevenly distributed on four citrus chromosomes. Chromosome 3 contained six CsSOD genes in a single gene cluster (*CsSOD01–06*), as defined by Holub's definition [42]. Four of the genes in the cluster appeared to have been involved in tandem duplication events. Although *CsSOD01* and *CsSOD06* were clearly related genes located on the same chromosome, their sequence similarities were low, and they were, there-

fore, not considered to be tandem duplicated genes. Chromosome 5 contained two CsSOD genes, *CsCOD07* and *CsCOD08*, that were far apart. Chromosome 7 contained four CsSOD genes (*CsSOD09–12*), of which *CsSOD09* and *CsSOD10* were tandem duplicates, while the remaining chromosome (Chromosome 8) contained only one CsSOD gene (*CsSOD13*) (Figure 2A). The gene structures of the CsSODs were then analyzed and visualized by GSDS (Figure 2B). As shown in the figure, *CsSOD01* contained the highest number of exons (14), while the exon numbers in the other genes varied between 5 and 14. The intron numbers were not consistent, and the introns also showed significant variations in length. Overall, the CsSOD genes, with the exceptions of *CsSOD09* and *CsSOD10*, showed a variety of intron/exon organizational patterns.

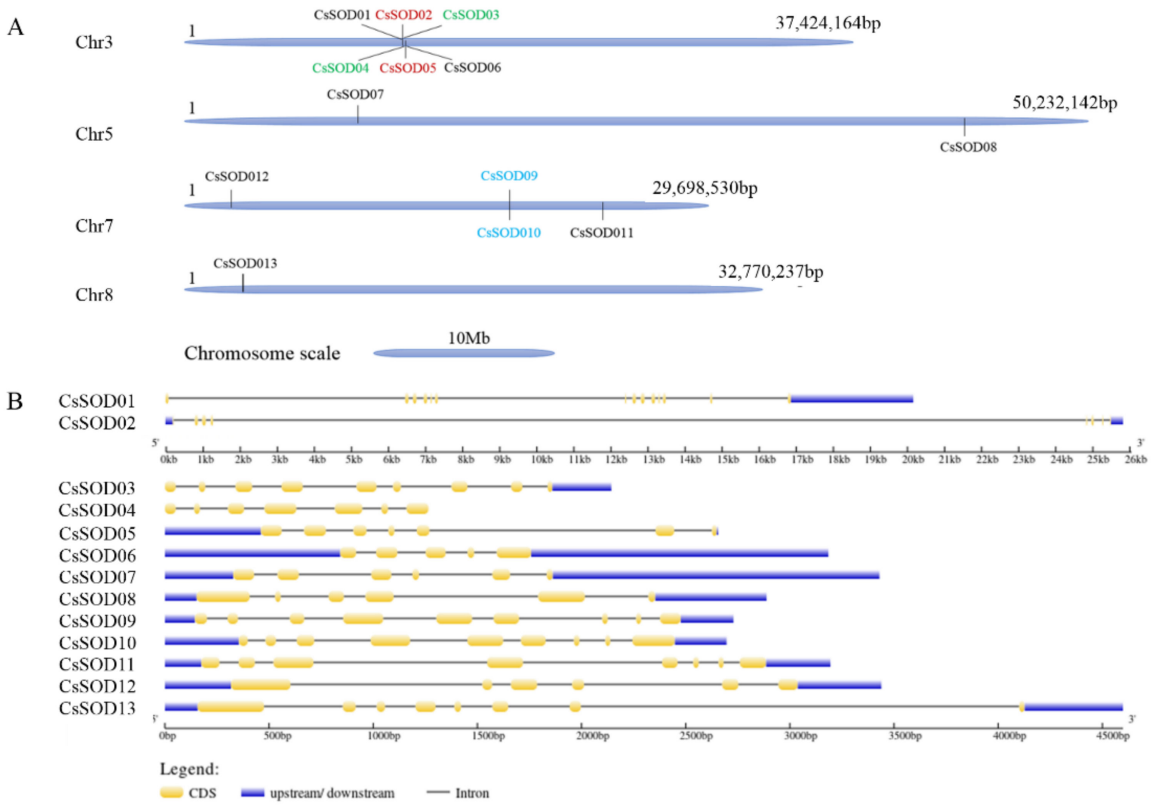

Figure 2. Chromosomal locations and intron/exon configurations of *CsSOD* genes. (**A**) Chromosomal distribution of CsSOD genes, visualized by MAPCHART V2.1. Chromosome numbers are shown on the left, while the chromosome lengths are shown on the right. Black lines indicate the positions of the CsSOD genes. Tandem duplicates are shown in the same color (apart from names shown in black). (**B**) Intron/exon configurations of CsSODs. Introns and exons are shown as yellow boxes and thin lines, respectively, while the UTRs are shown as blue boxes. The gene structures of CsSODs were visualized with GSDS V2.0.

3.3. Functional Domains of CsSODs

A Pfam analysis showed that the CsSODs fell into two major groups. The first group comprised Cu/ZnSODs and included nine members, each of which had one or two Cu/ZnSOD domains (*CsSOD01*, *02*, *03*, *04*, *05*, *06*, *07*, *08*, and *13*), while *CsSOD08* contained a heavy-metal-associated domain. The second group comprised the Fe-MnSODs. These enzymes contained an Fe/MnSOD alpha-hairpin domain and Fe/MnSOD C-terminal domains (*CsSOD9*, *10*, *11*, and *12*) (Figure 3A). The sequence alignment showed the conservation of these domains. The lengths of the domains, seen in Figure 3B, were 182–372 residues for the Cu/MnSOD domain, 166–264 residues for the Fe/MnSOD alpha-hairpin domain, and 270–391 residues for the Fe/MnSOD C-terminal domains (Figure 3B).

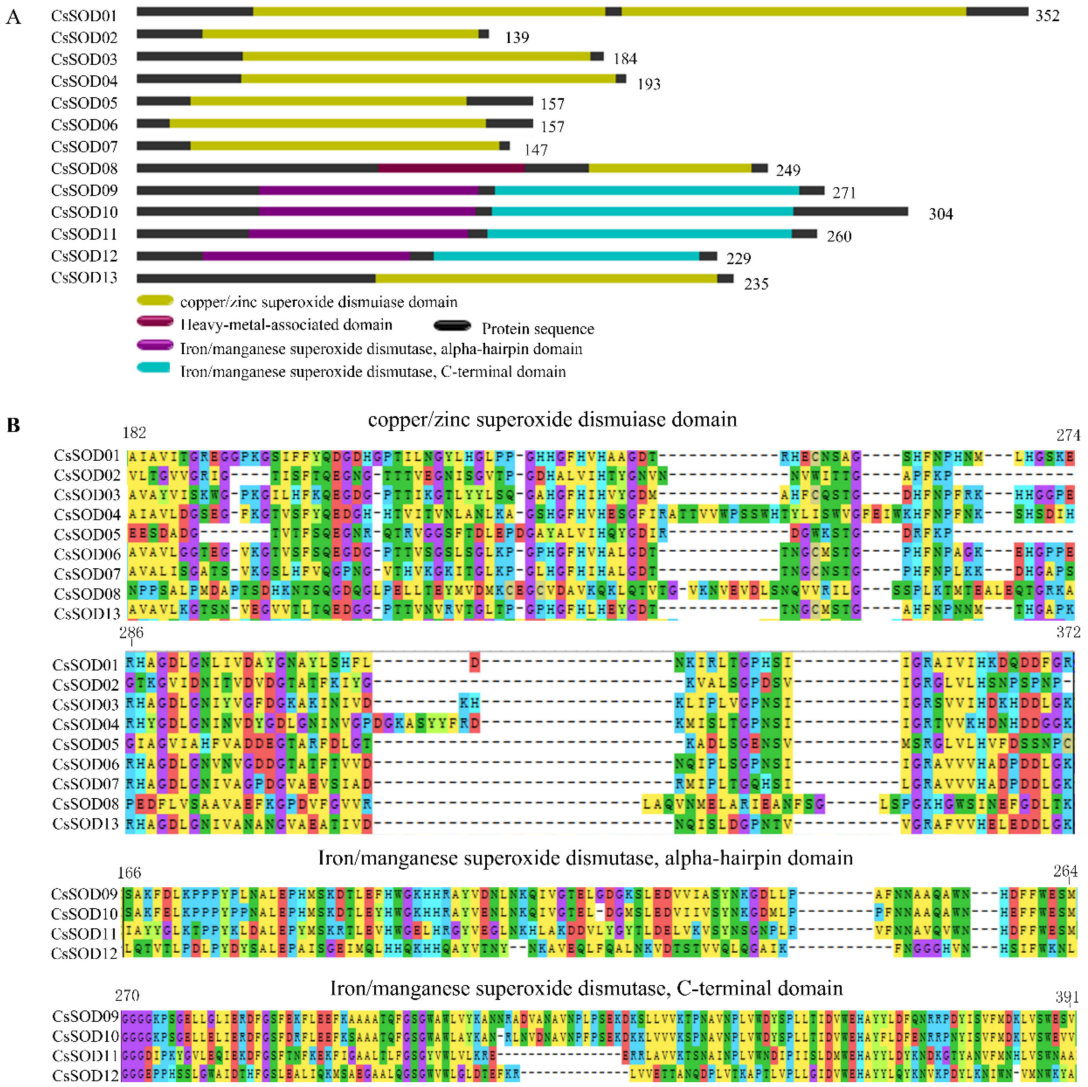

Figure 3. Functional domains of CsSODs. (**A**) The functional domains of CsSODs predicted by Pfam. Lines with different colors represent different functional domains. The numbers on the right represent the lengths of the protein sequences. (**B**) Alignments of CsSOD functional domains. Alignments were performed by ClustalW in MEGA V7.0.

3.4. Phylogenetic and Collinearity Analyses of the CsSOD Family in Arabidopsis and Citrus

An unrooted maximum-likelihood phylogenetic tree was constructed using 13 citrus sequences, 8 Arabidopsis sequences, and 9 tomato sequences (Figure 4A). According to their putative Arabidopsis orthologs, the SOD proteins fell into four clusters, I, II, III, and IV, although the homologs of the three species were not evenly distributed among the four clusters. The phylogenetic tree showed that the distribution of the CsSOD proteins in the tree was consistent with their metal cofactor types: Cu/ZnSODs (*CsSOD01*, *02*, *03*, *04*, *05*, *06*, *07*, and *13*) fell into group IV; Fe-MnSODs (*CsSOD09*, *10*, and *11*) were clustered in group I; *CsSOD12* belonged to group II; and *CsSOD08* and *SlSOD08* together formed group III. An examination of the citrus and Arabidopsis orthologs showed that three CsSODs had orthologs in Arabidopsis, and it is possible that these orthologous gene pairs share similar functions (Figure 4A). In addition, the three pairs of orthologs were verified by a collinearity analysis of the citrus and Arabidopsis SOD genes (Figure 4B).

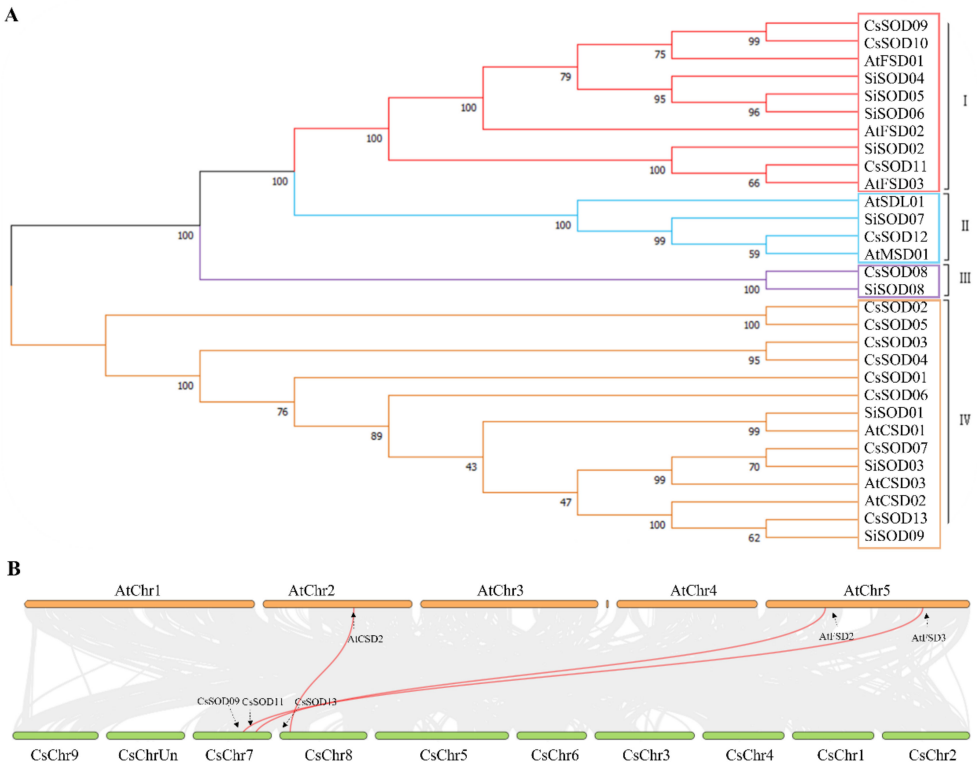

Figure 4. Phylogenetic and collinearity analyses of SOD family proteins in Arabidopsis and citrus. (**A**) Phylogenetic analysis of SOD family proteins in Arabidopsis and citrus. Sequences were aligned and the tree was compiled using the maximum-likelihood (ML) method in MEGA V7.0. *SiSOD01–09*: tomato SODs; *AtSOD01–08*: *Arabidopsis thaliana SODs*; *CsSOD01–13*: *C. sinensis* SODs. Branches are drawn to scale, with lengths corresponding to the number of substitutions per site. The four clusters, I, II, III, and IV, are represented by different line colors. (**B**) Collinearity analysis between CsSODs and AtSODs. TBTOOLS was used to analyze the comparative synteny between CsSODs and AtSODs. Red lines connect orthologs between citrus and Arabidopsis.

3.5. Conserved Motif Analysis of CsSOD Family Proteins

Eleven conserved protein motifs were identified in the citrus SOD proteins by MEME (Figure 5A,B). The CsSODs fell into two classes according to the Pfam domain predictions, with each class containing completely different motifs. Motif 2 was observed in Cu/ZnSODs (*CsSOD01–07* and *13*), and apart from *CsSOD01*, all other Cu/ZnSODs contained motif 6. Fe/MnSODs contained three motifs: motif 3, motif 4, and motif 10, while motifs 5, 7, and 9 were shared by the Fe/MnSODs, apart from *CsSOD12*.

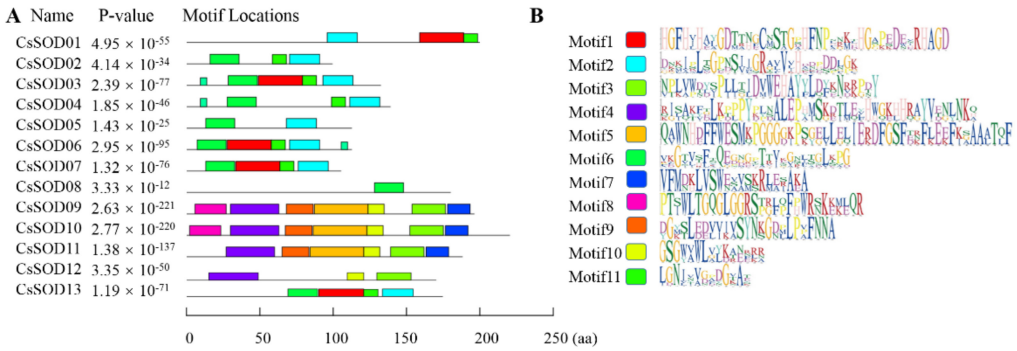

Figure 5. Conserved motif analysis of CsSOD family proteins. (**A**) Conserved protein motifs (minimum 6 and maximum 50 residues) in CsSOD family proteins analyzed by MEME. Different motifs are indicated by different color blocks. (**B**) Logo display of the 11 conserved motifs.

3.6. Analysis of Cis-Elements and Transcription Factor Binding Sites in Putative CsSOD Gene Promoters

To investigate the mechanisms by which CsSOD genes respond to stress signals and their regulation patterns, all the gene promoters (−2000 bp upstream of ATG) were analyzed using PlantCARE to identify possible cis-elements. The presence of transcription factor binding sites in the promoters was also investigated using JASPAR. The PlantCARE results showed that a relatively large number of light-responsive cis-elements, stress-related elements, and hormone-responsive cis-elements were present in the CsSOD promoters (Figure 6A). Hormone-responsive cis-elements were evenly distributed on the promoters of *CsSOD01–05* and *07*, positioned in the first 1000 bp of *CsSOD06*, and positioned in the last 1000 bp of *CsSOD08*, *09*, *12*, and *13* (Figure 6A). Notably, three plant hormone-response elements related to plant disease-resistance signals, namely, the JA response element (CGTCA-motif), ABA response element (ABRE), and SA response element (TCA-element), were unevenly distributed in the 13 genes. Between 1 and 14 ABRE sites were present on all CsSOD promoters, except for *CsSOD04* and *CsSOD13*. The CGTCA motif was not present on *CsSOD01*, *02*, *03*, *07*, or *12*. Although the TCA element is rarely found in this gene family, it was seen in *CsSOD01*, *02*, *08*, *09*, *11*, and *13* (Figure 6B). The binding sites were seen between −1900 and −1950 bp in *CsSOD06*, between −400 and −500 bp in *CsSOD07*, between −1400 and −1600 bp in *CsSOD11*, and between −800 and −900 bp in *CsSOD12*.

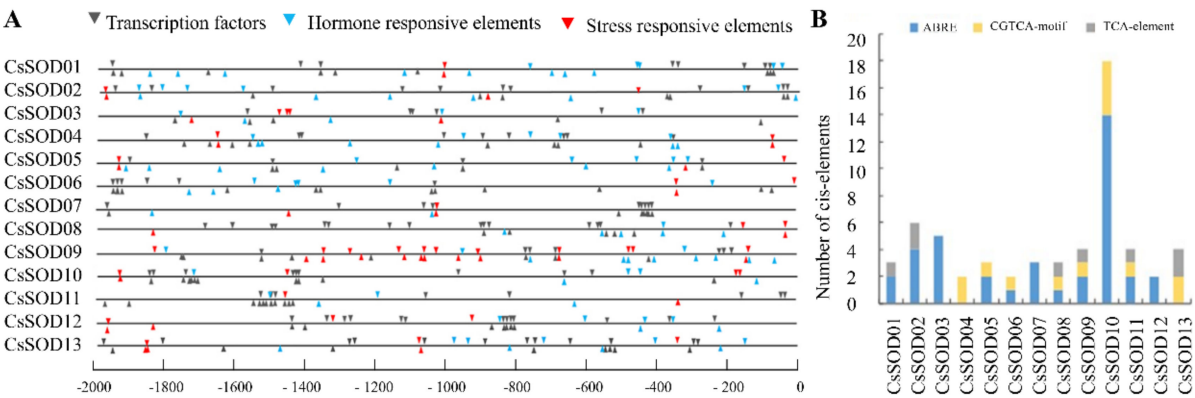

Figure 6. Putative cis-acting elements and transcription factor binding sites in the promotors of CsSOD genes. (**A**) Putative cis-acting elements were analyzed using PlantCARE, while the transcription factor binding sites were identified by JASPAR using a relative profile score threshold of 98%. Cis-elements with identical or similar functions are shown in the same color. (**B**) Hormone-responsive cis-elements in CsSOD promoter regions.

3.7. Predicted Protein–Protein Interaction (PPI) Network of CsSODs

The prediction of protein–protein interactions is useful for understanding the functions of proteins and unraveling their biological regulatory mechanisms. The predicted interaction partners and PPI networks for each CsSOD were compiled using STRING using the Arabidopsis PPI network as a reference. This showed that all the CsSODs were involved in a PPI network; *CsSOD01*, *02*, and *05* were in the same network, while *CsSOD09*, *10*, and *13* and *CsSOD03*, *04*, and *06* were in their own respective networks. It was also observed that CsSODs were predicted to interact with one another as well as share some interacting proteins. As shown in Figure 7, CsSODs were predicted to interact with 24 proteins, of which 7 interact only with *CsSOD08*. We speculated that these proteins may promote the functions of CsSODs. For example, MIA40, which was predicted to interact with Cu/ZnSODs is known to be involved in the mitochondrial oxidative folding of *Cu/ZnSOD01*, *02*, and *05* and the peroxisomal oxidative folding of the *Cu/ZnSOD CsSOD07*.

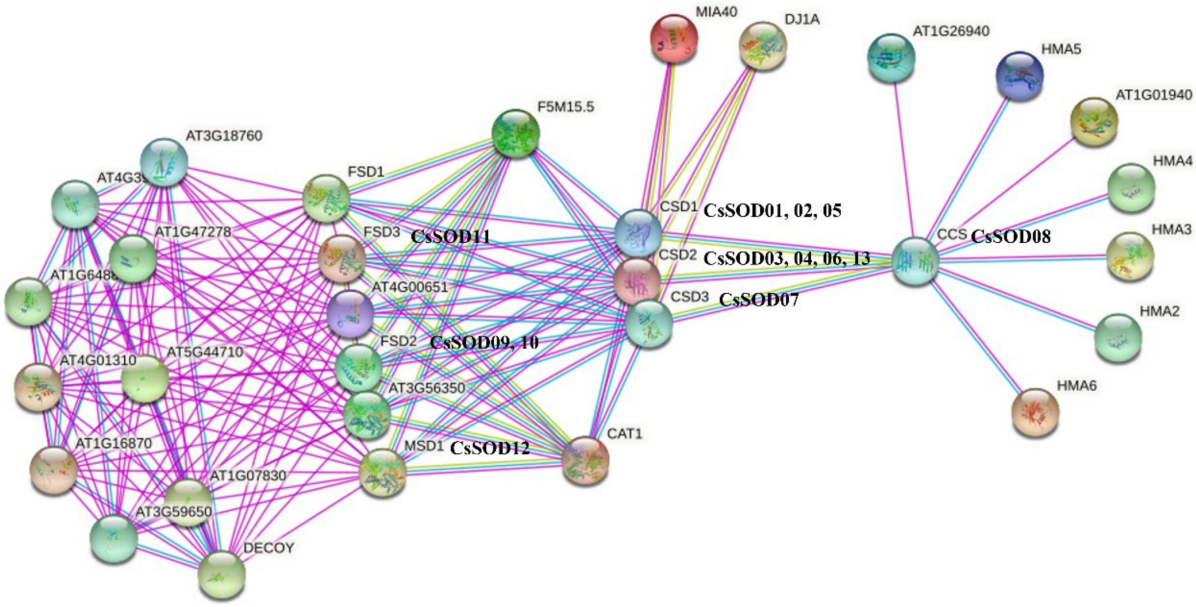

Figure 7. Predicted protein–protein interaction (PPI) networks of CsSODs. The PPI network was constructed using STRING V11. In the network, edge confidence was taken > 0.4, network nodes indicate proteins, and the patterns in the nodes are the three-dimensional structures of the proteins. The interacting protein names are shown in black, while CsSOD proteins are shown in bold black.

3.8. Expression Patterns of CsSODs Induced by Xcc

The effects of *Xcc* infection on the expression of CsSOD genes in Wanjincheng and Kumquat were investigated by qRT-PCR. It was found that CsSOD genes were either induced or inhibited during *Xcc* infection (Figure 8). In the canker-resistant Kumquat variety, *CsSOD01*, *02*, *03*, *04*, *05*, and *07* showed low expression 6 h after infection, while expression increased after 12 h, followed by reduced expression at the end of the experiment. This reduction, however, was not seen in *CsSOD04*. The expression of *CsSOD09* first increased and then decreased, while *CsSOD13* expression showed the opposite trend. In contrast, in the canker-sensitive Wanjincheng, *CsSOD07* and *CsSOD09–13* were all significantly downregulated, while *CsSOD01*, *03*, and *05* were most highly expressed at 12 h. Interestingly, the expression patterns of *CsSOD03* were similar in both Wanjincheng and Kumquat, while the expression of *CsSOD11* was completely different in the two varieties.

The comparison of both cultivars showed that the expression level of *CsSOD06* in Kumquat first increased and then decreased, reaching its highest level at 6 h, in contrast to a lack of significant change over time seen in Wanjincheng. At 6 h and 24 h, the expression of *CsSOD08* in Kumquat was significantly upregulated, with a trend opposite to that seen in Wanjincheng. Since Kumquat is a canker-resistant variety, we speculate that *CsSOD06* and *08* functions may be related to canker resistance.

3.9. CsSOD Expression Pattern Induced by Phytohormones

The expression profiles of CsSODs were further analyzed after treatment with the phytohormones SA, MeJA, and ABA. The expression of *CsSOD01*, *03*, *06*, *07*, *09*, *10*, *12*, and *13* was induced by SA in Kumquat, and *CsSOD02* and *04* were induced in Wanjincheng after 6 h. All the CsSOD genes were expressed and showed different expression patterns (Figure 9A). With ABA, the expression of *CsSOD13*, *12*, *10*, *05*, *06*, *07*, *03*, *02*, and *01* was upregulated in Kumquat at 36 h, and that of *CsSOD04*, *08*, and *CsSOD11* was upregulated at 48 h. The expression of *CsSOD02*, *05*, *09*, and *10* was downregulated in Wanjincheng. Notably, both *CsSOD06* and *CsSOD08* were gradually upregulated in both Kumquat and Wanjincheng (Figure 9B). After treatment with MeJA, the expression of *CsSOD13*, *12*, *10*,

06, *09*, and *01* was highest at 12 h in Kumquat, while that of *CsSOD03* and *04* was highest at 48 h in Wanjincheng. *CsSOD10* levels steadily increased, reaching their maximum at 48 h in Wanjincheng (Figure 9C). Overall, the expression of most of the CsSOD genes was significantly altered by phytohormones.

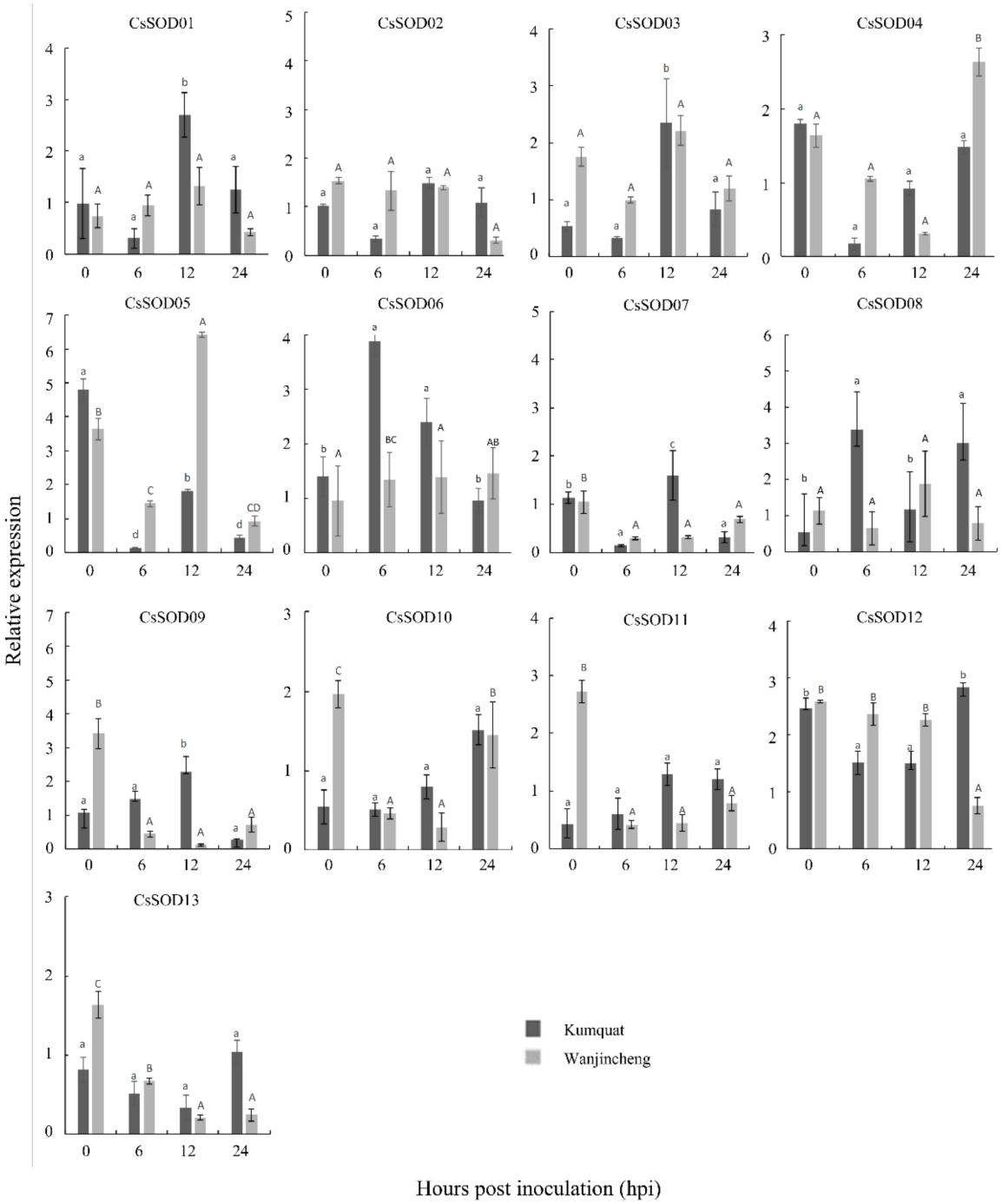

Figure 8. Expression profiles of CsSODs during *Xcc* infection. Leaf samples were taken at 0, 6, 12, and 24 hpt. Different letters on the bars indicate significant differences ($p < 0.05$) based on Duncan's LSD multiple range test. Data are means ± SDs of three qRT-PCR experiments and three biological replicates.

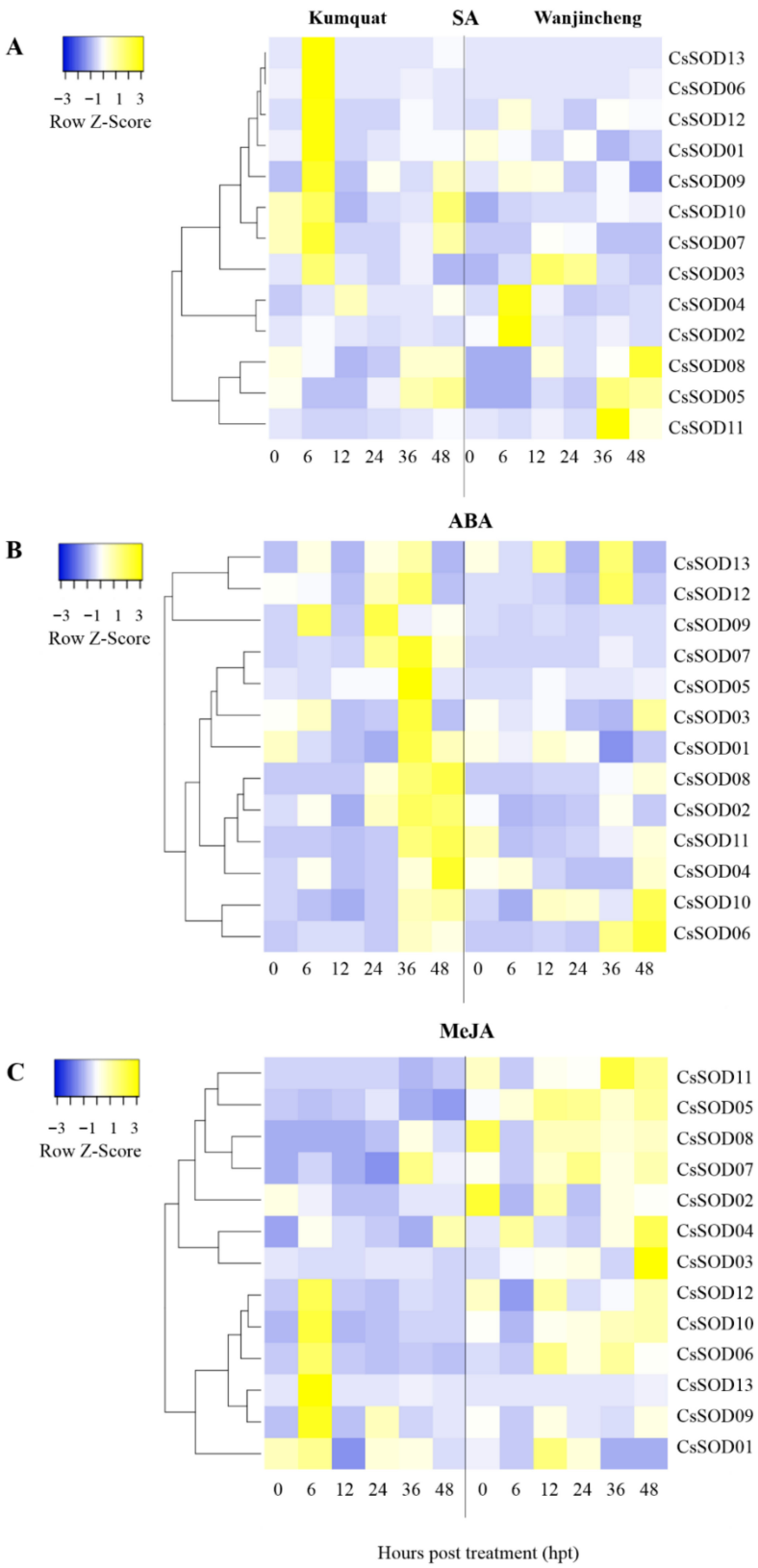

Figure 9. Expression profiles of CsSOD genes in response to phytohormones. (**A**) Expression after SA treatment. (**B**) Expression after ABA treatment. (**C**) Expression after MeJA treatment. The online site Heatmapper was used for drawing. Changes from blue to yellow indicate changes in relative expression levels.

3.10. Transient Expression of CsSOD06 and CsSOD08

In plants, the rapid generation of ROS, including the superoxide anion (OFR) and H_2O_2, indicates the recognition of pathogenic infection. H_2O_2 is more stable than OFR and can not only damage biological macromolecules but also serves as a signaling molecule itself [43]. OFR is an early type of ROS, and its production is a reflection of cellular damage and the strength of resistance under adverse conditions [44]. As shown in Figure 10, *CsSOD06* and *08* may be associated with canker resistance in Kumquat. We constructed overexpression vectors for *CsSOD06* and *08* for transient expression in the leaves of Wanjincheng. After five days of Agrobacterium infection, there was a significant increase in the expression of *CsSOD06* and *08* (Figure 10A). Both the H_2O_2 content and SOD activity increased significantly in leaves overexpressing *CsSOD06* and *08*, while the OFR content decreased compared with pLGN leaves (Figure 10B–D). These results suggest that the ROS content of citrus leaves was affected by the overexpression of *CsSOD06* and *08*. In addition, the influence of *CsSOD08* was greater than that of *CsSOD06*. Considering that *CsSOD06* and *CsSOD08* are induced and expressed by *Xcc* and phytohormones in citrus, these findings suggest that they participate in resistance and susceptibility responses by regulating the ROS balance.

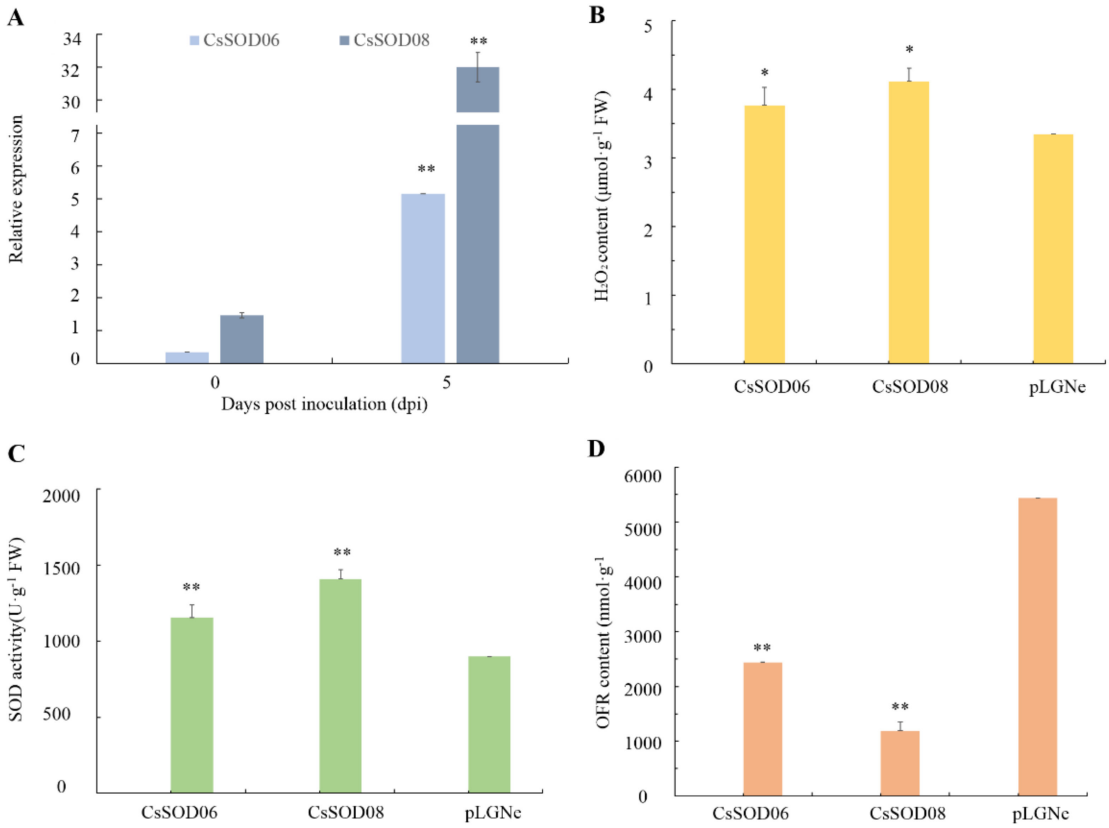

Figure 10. Transient expression of *CsSOD06* and *CsSOD08*. (**A**) Expression level of *CsSOD06* and *CsSOD08* in Wanjincheng leaves five days after transient expression. (**B**) H_2O_2 content in *CsSOD06*- and *CsSOD08*-overexpressing cells. (**C**) SOD activities in *CsSOD06*- and *CsSOD08*-overexpressing cells. (**D**) OFR contents in *CsSOD06*- and *CsSOD08*-overexpressing cells. In (**A**–**D**), *p* indicates the pLGNe vector. All experiments were repeated a minimum of three times; each value represents the mean ± SD. * indicates significant differences ($p \leq 0.05$) and ** indicates extremely significant differences ($p \leq 0.01$).

4. Discussion

The number of SOD genes varies in different species. For example, there are 25, 8, 29, and 18 SOD genes in banana [45], *Dendrobium catenatum* [46], juncea, and rapa [47], respectively. In the current study, we identified a total of 13 CsSODs in the *C. sinensis* genome, including 4 Fe/MnSODs and 9 Cu/ZnSODs [48].

The promoter regions of eukaryotic genes essentially consist of two parts. The first part is the core promoter region containing the transcriptional initiation site and the core promoter element (TATA-box). The second part is the region containing upstream regulatory elements, including upstream enhancer elements and various response elements. These elements in the promoter determine the specificity and degree of gene transcription [49]. Three major classes of cis-elements were observed in the promoters of the citrus *SOD* genes. The first type was stress-responsive, including TCA elements, LTRs, TC-rich repeats, and Box-W1s that respond to drought, low temperature, and salt stress, respectively [50–52]. The second type was light-responsive; research has shown that certain *SOD* genes may be light-responsive [5,53]. The accumulation of Cu/ZnSOD and FeSOD transcripts has been found to increase in tobacco, Arabidopsis, and rice when exposed to light stress [5]. SOD enzyme activities have also been shown to decrease in *Chrysanthemum indicum* under conditions of reduced light [54]. The third type is hormone-responsive. Hormone-responsive transcription factors act by interacting with their corresponding cis-elements to modulate the transcription of target genes under stress conditions [55]. It was found that the expression of the CsSODs increased between 24 h and 48 h in Kumquat, including the expression of *CsSOD04* and *CsSOD13*, which lack ABRE (Figure 6). This suggests that CsSODs may participate in ABA responses and may cooperate with other regulatory mechanisms in response to ABA. For example, an ABA-inducible germin-like protein CpGLP1 has been found to have SOD activity [56], and activation of the ABA signaling pathway by γ-aminobutyric acid (GABA) increased the activities of SOD [57]. In addition, upregulation of the *A. thaliana* (*At*) cold-inducible gene (*AtCBF2*) and desiccation-responsible transcription factors (*AtRD29A/B*) were observed in *AtSOD* transgenic plants after treatment with ABA. In addition to ABA, SOD genes have also been found to respond to gibberellin A and auxin in tobacco [58] and to MeJA and SA in *Bletilla striata* [59]. We demonstrated that MeJA, ABA, and SA modulate the expression of CsSODs and suggest that CsSODs are likely to participate in phytohormonal signaling pathways.

The different domains observed in CsSODs suggest that the proteins may have different functions (Figure 3). Previous studies have reported that the 5′ regions of SOD genes play important roles in the function of these enzymes [60]. The highly conserved domain in the CsSOD proteins may be responsible for protein interactions. Potential interaction partners of the CcSODs were predicted, and their associated functions were analyzed; further investigation of these predicted interactions will provide more information about the function of the CsSOD gene family. The PPI networks also demonstrated the role of protein interactions in the regulation of plant physiology, including interactions with F5M15.5 and CAT1 that protect cells from the toxic effects of H_2O_2 (Figure 7). CAT1 belongs to the catalase family, is found in almost all aerobically respiring organisms, and protects cells from the toxic effects of hydrogen peroxide [61]. It has been suggested that CAT1 may interact with all CsSOD proteins except for *CsSOD08*, as ROS clearance is performed by both SOD and CAT (CAT1 and CDS2) [62]. The expression levels of CAT1 and SOD increase or decrease simultaneously when plants encounter abiotic stress [63–65].

As described, CsSODs play essential roles in a plant's defense against stress, including bacterial infection. To clarify the potential functions of CsSODs, this study analyzed their expression patterns in response to *Xcc* infection, contrasting them with the response to hormones and finding that most CcSOD genes respond to both pathogens and hormonal stress (Figures 8 and 9). Ten CsSODs were found to be upregulated by MeJA in Wanjincheng, while *CsSOD06* and *08* were upregulated in response to ABA in both Wanjincheng and Kumquat, indicating that *Xcc* infection led to distinctive expression profiles for most of the CsSODs. These findings suggest that different CsSODs *associated* with different citrus

varieties may have different roles in phytohormonal signaling pathways. Based on these results, the CDS of *CsSOD06* and *08* without the stop codons were amplified, inserted into pLGNe vectors to construct pLGN-*CsSOD06* and *08* plasmids, and transformed into citrus leaves by Agrobacterium injection. A previous report described the levels of endogenous H_2O_2 in peroxisomes, enhancing our knowledge of ROS [66]. In our study, the H_2O_2 contents were found to increase, while the OFR contents decreased, suggesting that the ROS signaling pathway includes the rapid generation and removal of various forms of ROS to maintain overall ROS homeostasis [67]. The expression of CsSODs in the canker-sensitive Wanjincheng and canker-resistant Kumquat varieties induced by *Xcc* demonstrated the relationship between CsSODs and CBC. Therefore, we infer that the expression of CsSOD genes may affect the resistance of citrus to CBC by reprogramming ROS homeostasis.

5. Conclusions

Taken together, we provide a comprehensive analysis of citrus SOD enzymes using phylogenetic, motif, and collinearity analyses and comparisons with Arabidopsis homologs to explore the evolution and functions of this important gene family. The expression of the CsSOD genes in response to Xcc infection and phytohormone treatment was measured by qRT-PCR.

Importantly, the study laid the groundwork for the utilization of citrus SOD genes. Further studies on the screening of disease resistance genes will be developed based on this study, and other plants will be studied in related fields based on these findings. CsSODs are potential candidate genes for CBC research, and there are new ideas for combating CBC based on the results of this study. This is beneficial for the healthy development of citrus industry, but more research is needed to fully understand their roles.

Supplementary Materials: The following supporting information can be downloaded at: https://www.mdpi.com/article/10.3390/agriculture12081254/s1, Supplementary Table S1: Primers used in this study. CPBD: Citrus Pan-genome to Breeding Database (http://citrus.hzau.edu.cn/, accessed on 13 October 2021); *: KpnI and EcoRI restriction enzyme site and protective base included. **: KpnI and BamHI restriction enzyme site and protective base, including primers used for qRT-PCR, were designed using NCBI Primer BLAST with *Citrus sinensis* for the specificity check; Table S2: The sequences of SODs in *Citrus sinensis*. CPBD: Citrus Pan-Genome to Breeding Database; *: 5′ and 3′ untranslated regions (UTRs) included, if any; **: 2000 bp upstream of ATG; Table S3: The protein sequences of *SODs* in *Citrus sinensis*, tomato, and *A. thaliana*. CPBD: Citrus Pan-genome to Breeding Database (http://citrus.hzau.edu.cn/, accessed on 14 October 2021).

Author Contributions: Q.L. and Y.H. designed the experiments; W.Y., Q.Y., J.F. (Jia Fu) and X.Q. performed the experiments; W.Y., B.X., C.Z., X.H., J.F. (Jie Fan) and S.C. analyzed the data; W.Y. and Q.L. wrote this article. All authors have read and agreed to the published version of the manuscript.

Funding: This study was funded by the Natural Science Foundation of Chongqing (cstc2020jcyj-msxmX1064), Earmarked Funds for the China Agriculture Research System (CARS-26), and the Guangxi Science and Technology Key Project (GuiKeAA18118046-6).

Data Availability Statement: Not applicable.

Conflicts of Interest: The authors declare no conflict of interest.

References

1. Snowdon, R.J.; Wittkop, B.; Chen, T.W.; Stahl, A. Crop adaptation to climate change as a consequence of long-term breeding. *Theor. Appl. Genet.* **2021**, *134*, 1613–1623. [CrossRef] [PubMed]
2. Wang, T.; Song, H.; Zhang, B.; Lu, Q.; Liu, Z.; Zhang, S.; Guo, R.; Wang, C.; Zhao, Z.; Liu, J.; et al. Genome-wide identification, characterization, and expression analysis of superoxide dismutase (SOD) genes in foxtail millet (*Setaria italica* L.). *3 Biotech.* **2018**, *8*, 486. [CrossRef] [PubMed]
3. Feng, K.; Yu, J.; Cheng, Y.; Ruan, M.; Wang, R.; Ye, Q.; Zhou, G.; Li, Z.; Yao, Z.; Yang, Y.; et al. The SOD Gene Family in Tomato: Identification, Phylogenetic Relationships, and Expression Patterns. *Front. Plant Sci.* **2016**, *7*, 1279. [CrossRef] [PubMed]
4. Zang, Y.; Chen, J.; Li, R.; Shang, S.; Tang, X. Genome-wide analysis of the superoxide dismutase (SOD) gene family in *Zostera marina* and expression profile analysis under temperature stress. *PeerJ* **2020**, *8*, e9063. [CrossRef]

5. Wang, W.; Zhang, X.; Deng, F.; Yuan, R.; Shen, F. Genome-wide characterization and expression analyses of superoxide dismutase (SOD) genes in *Gossypium hirsutum*. *BMC Genom.* **2017**, *18*, 376. [CrossRef]
6. Li, Z.; Han, X.; Song, X.; Zhang, Y.; Jiang, J.; Han, Q.; Liu, M.; Qiao, G.; Zhuo, R. Overexpressing the *Sedum alfredii* Cu/Zn Superoxide Dismutase Increased Resistance to Oxidative Stress in Transgenic *Arabidopsis*. *Front. Plant Sci.* **2017**, *8*, 1010. [CrossRef]
7. Huo, C.; He, L.; Yu, T.; Ji, X.; Li, R.; Zhu, S.; Zhang, F.; Xie, H.; Liu, W. The Superoxide Dismutase Gene Family in *Nicotiana tabacum*: Genome-Wide Identification, Characterization, Expression Profiling and Functional Analysis in Response to Heavy Metal Stress. *Front. Plant Sci.* **2022**, *13*, 904105. [CrossRef]
8. Melicher, P.; Dvorak, P.; Krasylenko, Y.; Shapiguzov, A.; Kangasjarvi, J.; Samaj, J.; Takac, T. Arabidopsis Iron Superoxide Dismutase FSD1 Protects Against Methyl Viologen-Induced Oxidative Stress in a Copper-Dependent Manner. *Front. Plant Sci.* **2022**, *13*, 823561. [CrossRef]
9. Dvorak, P.; Krasylenko, Y.; Ovecka, M.; Basheer, J.; Zapletalova, V.; Samaj, J.; Takac, T. FSD1: Developmentally-regulated plastidial, nuclear and cytoplasmic enzyme with anti-oxidative and osmoprotective role. *Plant Cell Environ.* **2020**. [CrossRef]
10. Lu, X.; Guan, Q.; Zhu, J. Downregulation of CSD2 by a heat-inducible miR398 is required for thermotolerance in *Arabidopsis*. *Plant Signal. Behav.* **2013**, *8*, e24952. [CrossRef]
11. Sunkar, R.; Kapoor, A.; Zhu, J.K. Posttranscriptional induction of two Cu/Zn superoxide dismutase genes in *Arabidopsis* is mediated by downregulation of miR398 and important for oxidative stress tolerance. *Plant Cell* **2006**, *18*, 2051–2065. [CrossRef]
12. Gallie, D.R.; Chen, Z. Chloroplast-localized iron superoxide dismutases FSD2 and FSD3 are functionally distinct in *Arabidopsis*. *PLoS ONE* **2019**, *14*, e0220078. [CrossRef]
13. Wang, F.Z.; Wang, Q.B.; Kwon, S.Y.; Kwak, S.S.; Su, W.A. Enhanced drought tolerance of transgenic rice plants expressing a pea manganese superoxide dismutase. *J. Plant Physiol.* **2005**, *162*, 465–472. [CrossRef]
14. Shafi, A.; Gill, T.; Sreenivasulu, Y.; Kumar, S.; Ahuja, P.S.; Singh, A.K. Improved callus induction, shoot regeneration, and salt stress tolerance in *Arabidopsis* overexpressing superoxide dismutase from *Potentilla atrosanguinea*. *Protoplasma* **2015**, *252*, 41–51. [CrossRef]
15. Wang, Y.C.; Qu, G.Z.; Li, H.Y.; Wu, Y.J.; Wang, C.; Liu, G.F.; Yang, C.P. Enhanced salt tolerance of transgenic poplar plants expressing a manganese superoxide dismutase from *Tamarix androssowii*. *Mol. Biol. Rep.* **2010**, *37*, 1119–1124. [CrossRef]
16. Lin, K.H.; Sei, S.C.; Su, Y.H.; Chiang, C.M. Overexpression of the *Arabidopsis* and winter squash superoxide dismutase genes enhances chilling tolerance via ABA-sensitive transcriptional regulation in transgenic *Arabidopsis*. *Plant Signal. Behav.* **2019**, *14*, 1685728. [CrossRef]
17. Li, Y.; Cao, X.L.; Zhu, Y.; Yang, X.M.; Zhang, K.N.; Xiao, Z.Y.; Wang, H.; Zhao, J.H.; Zhang, L.L.; Li, G.B.; et al. Osa-miR398b boosts H_2O_2 production and rice blast disease-resistance via multiple superoxide dismutases. *New Phytol.* **2019**, *222*, 1507–1522. [CrossRef]
18. Cabrejos, D.A.L.; Alexandrino, A.V.; Pereira, C.M.; Mendonca, D.C.; Pereira, H.D.; Novo-Mansur, M.T.M.; Garratt, R.C.; Goto, L.S. Structural characterization of a pathogenicity-related superoxide dismutase codified by a probably essential gene in *Xanthomonas citri* subsp. *citri*. *PLoS ONE* **2019**, *14*, e0209988. [CrossRef]
19. Diaz-Vivancos, P.; Rubio, M.; Mesonero, V.; Periago, P.M.; Barcelo, A.R.; Martinez-Gomez, P.; Hernandez, J.A. The apoplastic antioxidant system in *Prunus*: Response to long-term plum pox virus infection. *J. Exp. Bot.* **2006**, *57*, 3813–3824. [CrossRef]
20. Fan, W.W.; Wang, L.A.; Chun, H.M.; Wen, W.D.; Yun, C.L.; Zi, H.L.; Yin, S.J.; Geng, J.Y.; Zhang, X.Y. The Influence of the *Verticillium dahliae* Kleb Infection on the Anti-Enzyme Inside the Body of the Cotton with Different Root Injured Degree. *Agric. Sci. China* **2007**, *6*, 816–824. [CrossRef]
21. Li, T.; Huang, M.C.; Zhang, D.D.; Ran, L.; Chen, J.Y.; Sun, W.X.; Qiu, N.W.; Dai, X.F. Extracellular superoxide dismutase *VdSOD5* is required for virulence in *Verticillium dahliae*. *J. Integr. Agric.* **2021**, *20*, 1858–1870.
22. Faize, M.; Faize, L.; Alburquerque, N.; Venisse, J.S.; Burgos, L. Hydrogen peroxide generated by over-expression of cytosolic superoxide dismutase in transgenic plums enhances bacterial canker resistance and modulates plant defence responses. *Mol. Biol. Rep.* **2020**, *47*, 5889–5901. [CrossRef]
23. Coaker, G.L.; Willard, B.; Kinter, M.; Stockinger, E.J.; Francis, D.M. Proteomic analysis of resistance mediated by Rcm 2.0 and Rcm 5.1, two loci controlling resistance to bacterial canker of tomato. *Mol. Plant-Microbe Interact.* **2004**, *17*, 1019–1028. [CrossRef]
24. Sun, L.; Ke, F.; Nie, Z.; Wang, P.; Xu, J. Citrus Genetic Engineering for Disease Resistance: Past, Present and Future. *Int. J. Mol. Sci.* **2019**, *20*, 5256. [CrossRef]
25. Zhang, J.; Huguet-Tapia, J.C.; Hu, Y.; Jones, J.; Wang, N.; Liu, S.; White, F.F. Homologues of CsLOB1 in citrus function as disease susceptibility genes in citrus canker. *Mol. Plant Pathol.* **2017**, *18*, 798–810. [CrossRef]
26. Xu, Q.; Chen, L.L.; Ruan, X.; Chen, D.; Zhu, A.; Chen, C.; Bertrand, D.; Jiao, W.B.; Hao, B.H.; Lyon, M.P.; et al. The draft genome of sweet orange (*Citrus sinensis*). *Nat. Genet.* **2013**, *45*, 59–66. [CrossRef]
27. Wang, J.; Chen, D.; Lei, Y.; Chang, J.W.; Hao, B.H.; Xing, F.; Li, S.; Xu, Q.; Deng, X.X.; Chen, L.L. *Citrus sinensis* annotation project (CAP): A comprehensive database for sweet orange genome. *PLoS ONE* **2014**, *9*, e87723. [CrossRef]
28. Reiser, L.; Subramaniam, S.; Li, D.; Huala, E. Using the *Arabidopsis* Information Resource (TAIR) to Find Information About *Arabidopsis* Genes. *Curr. Protoc. Bioinform.* **2017**, *60*, 1.11.1–1.11.45. [CrossRef]
29. Duvaud, S.; Gabella, C.; Lisacek, F.; Stockinger, H.; Ioannidis, V.; Durinx, C. Expasy, the Swiss Bioinformatics Resource Portal, as designed by its users. *Nucleic Acids Res.* **2021**, *49*, W216–W227. [CrossRef]

30. Tamura, K.; Peterson, D.; Peterson, N.; Stecher, G.; Nei, M.; Kumar, S. MEGA5: Molecular evolutionary genetics analysis using maximum likelihood, evolutionary distance, and maximum parsimony methods. *Mol. Biol. Evol.* **2011**, *28*, 2731–2739. [CrossRef]
31. Hu, B.; Jin, J.; Guo, A.Y.; Zhang, H.; Luo, J.; Gao, G. GSDS 2.0: An upgraded gene feature visualization server. *Bioinformatics* **2015**, *31*, 1296–1297. [CrossRef] [PubMed]
32. Bailey, T.L.; Boden, M.; Buske, F.A.; Frith, M.; Grant, C.E.; Clementi, L.; Ren, J.; Li, W.W.; Noble, W.S. MEME SUITE: Tools for motif discovery and searching. *Nucleic Acids Res.* **2009**, *37*, W202–W208. [CrossRef] [PubMed]
33. Voorrips, R.E. MapChart: Software for the graphical presentation of linkage maps and QTLs. *J. Hered.* **2002**, *93*, 77–78. [CrossRef] [PubMed]
34. Yu, C.S.; Chen, Y.C.; Lu, C.H.; Hwang, J.K. Prediction of protein subcellular localization. *Proteins* **2006**, *64*, 643–651. [CrossRef]
35. El-Gebali, S.; Mistry, J.; Bateman, A.; Eddy, S.R.; Luciani, A.; Potter, S.C.; Qureshi, M.; Richardson, L.J.; Salazar, G.A.; Smart, A.; et al. The Pfam protein families database in 2019. *Nucleic Acids Res.* **2019**, *47*, D427–D432. [CrossRef]
36. Lescot, M.; Dehais, P.; Thijs, G.; Marchal, K.; Moreau, Y.; Van de Peer, Y.; Rouze, P.; Rombauts, S. PlantCARE, a database of plant cis-acting regulatory elements and a portal to tools for in silico analysis of promoter sequences. *Nucleic Acids Res.* **2002**, *30*, 325–327. [CrossRef]
37. Szklarczyk, D.; Morris, J.H.; Cook, H.; Kuhn, M.; Wyder, S.; Simonovic, M.; Santos, A.; Doncheva, N.T.; Roth, A.; Bork, P.; et al. The STRING database in 2017: Quality-controlled protein-protein association networks, made broadly accessible. *Nucleic Acids Res.* **2017**, *45*, D362–D368. [CrossRef]
38. Chen, C.; Chen, H.; Zhang, Y.; Thomas, H.R.; Frank, M.H.; He, Y.; Xia, R. TBtools: An Integrative Toolkit Developed for Interactive Analyses of Big Biological Data. *Mol. Plant* **2020**, *13*, 1194–1202. [CrossRef]
39. Castro-Mondragon, J.A.; Riudavets-Puig, R.; Rauluseviciute, I.; Berhanu Lemma, R.; Turchi, L.; Blanc-Mathieu, R.; Lucas, J.; Boddie, P.; Khan, A.; Manosalva Perez, N.; et al. JASPAR 2022: The 9th release of the open-access database of transcription factor binding profiles. *Nucleic Acids Res.* **2022**, *50*, D165–D173. [CrossRef]
40. Babicki, S.; Arndt, D.; Marcu, A.; Liang, Y.; Grant, J.R.; Maciejewski, A.; Wishart, D.S. Heatmapper: Web-enabled heat mapping for all. *Nucleic Acids Res.* **2016**, *44*, W147–W153. [CrossRef]
41. Livak, K.J.; Schmittgen, T.D. Analysis of relative gene expression data using real-time quantitative PCR and the 2(-Delta Delta C(T)) Method. *Methods* **2001**, *25*, 402–408. [CrossRef]
42. Holub, E.B. The arms race is ancient history in Arabidopsis, the wildflower. *Nat. Rev. Genet.* **2001**, *2*, 516–527. [CrossRef]
43. Tian, S.; Wang, X.; Li, P.; Wang, H.; Ji, H.; Xie, J.; Qiu, Q.; Shen, D.; Dong, H. Plant Aquaporin AtPIP1;4 Links Apoplastic H_2O_2 Induction to Disease Immunity Pathways. *Plant Physiol.* **2016**, *171*, 1635–1650. [CrossRef]
44. Ren, X.; Wang, M.; Wang, Y.; Huang, A. Superoxide anion generation response to wound in Arabidopsis hypocotyl cutting. *Plant Signal. Behav.* **2021**, *16*, 1848086. [CrossRef]
45. Feng, X.; Lai, Z.; Lin, Y.; Lai, G.; Lian, C. Genome-wide identification and characterization of the superoxide dismutase gene family in *Musa acuminata* cv. Tianbaojiao (AAA group). *BMC Genom.* **2015**, *16*, 823. [CrossRef]
46. Gomez, J.M.; Hernandez, J.A.; Jimenez, A.; del Rio, L.A.; Sevilla, F. Differential response of antioxidative enzymes of chloroplasts and mitochondria to long-term NaCl stress of pea plants. *Free. Radic. Res.* **1999**, *31* (Suppl. S1), S11–S18. [CrossRef]
47. Huang, H.; Wang, H.; Tong, Y.; Wang, Y. Insights into the Superoxide Dismutase Gene Family and Its Roles in *Dendrobium catenatum* under Abiotic Stresses. *Plants* **2020**, *9*, 1452. [CrossRef]
48. Parker, M.W.; Blake, C.C. Iron-and manganese-containing superoxide dismutases can be distinguished by analysis of their primary structures. *FEBS Lett.* **1988**, *229*, 377–382. [CrossRef]
49. Lu, Y.; Chen, X.; Wu, Y.; Wang, Y.; He, Y.; Wu, Y. Directly transforming PCR-amplified DNA fragments into plant cells is a versatile system that facilitates the transient expression assay. *PLoS ONE* **2013**, *8*, e57171. [CrossRef]
50. Verma, D.; Lakhanpal, N.; Singh, K. Genome-wide identification and characterization of abiotic-stress responsive SOD (superoxide dismutase) gene family in *Brassica juncea* and *B. rapa*. *BMC Genom.* **2019**, *20*, 227. [CrossRef]
51. Wu, G.; Wilen, R.W.; Robertson, A.J.; Gusta, L.V. Isolation, chromosomal localization, and differential expression of mitochondrial manganese superoxide dismutase and chloroplastic copper/zinc superoxide dismutase genes in wheat. *Plant Physiol.* **1999**, *120*, 513–520. [CrossRef]
52. Baek, K.H.; Skinner, D.Z. Alteration of antioxidant enzyme gene expression during cold acclimation of near-isogenic wheat lines. *Plant Sci.* **2003**, *165*, 1221–1227. [CrossRef]
53. Gupta, A.S.; Heinen, J.L.; Holaday, A.S.; Burke, J.J.; Allen, R.D. Increased resistance to oxidative stress in transgenic plants that overexpress chloroplastic Cu/Zn superoxide dismutase. *Proc. Natl. Acad. Sci. USA* **1993**, *90*, 1629–1633. [CrossRef]
54. Xuan, H.M.; Shi, H.Z.; Guo, Q.S.; Zhang, H.N.; Lei, M.; Wang, C.L. Effects of light intensity on physio-biochemical characteristics of *Chrysanthemum indicum*. *Zhongguo Zhong Yao Za Zhi* **2020**, *45*, 1620–1626.
55. Wang, S.; Bai, Y.; Shen, C.; Wu, Y.; Zhang, S.; Jiang, D.; Guilfoyle, T.J.; Chen, M.; Qi, Y. Auxin-related gene families in abiotic stress response in *Sorghum bicolor*. *Funct. Integr. Genom.* **2010**, *10*, 533–546. [CrossRef]
56. Giarola, V.; Chen, P.; Dulitz, S.J.; Konig, M.; Manduzio, S.; Bartels, D. The dehydration- and ABA-inducible germin-like protein CpGLP1 from *Craterostigma plantagineum* has SOD activity and may contribute to cell wall integrity during desiccation. *Planta* **2020**, *252*, 84. [CrossRef]
57. Liu, C.; Wang, H.; Zhang, X.; Ma, F.; Guo, T.; Li, C. Activation of the ABA Signal Pathway Mediated by GABA Improves the Drought Resistance of Apple Seedlings. *Int. J. Mol. Sci.* **2021**, *22*, 12676. [CrossRef]

58. Kurepa, J.; Herouart, D.; Van Montagu, M.; Inze, D. Differential expression of CuZn- and Fe-superoxide dismutase genes of tobacco during development, oxidative stress, and hormonal treatments. *Plant Cell Physiol.* **1997**, *38*, 463–470. [CrossRef]
59. Yang, J.W.; Wang, K.C.; Liang, J.Y.; Wang, J.; Xia, T.S.; Liang, Y.F. Effects of exogenous MeJA, SA and two kinds of endophytic fungi on physiology and total phenols content of seedlings of Bletilla striata. *Zhongguo Zhong Yao Za Zhi* **2016**, *41*, 2794–2801.
60. Fink, R.C.; Scandalios, J.G. Molecular evolution and structure–function relationships of the superoxide dismutase gene families in angiosperms and their relationship to other eukaryotic and prokaryotic superoxide dismutases. *Arch. Biochem. Biophys.* **2002**, *399*, 19–36. [CrossRef]
61. Zhao, Q.; Zhou, L.; Liu, J.; Cao, Z.; Du, X.; Huang, F.; Pan, G.; Cheng, F. Involvement of CAT in the detoxification of HT-induced ROS burst in rice anther and its relation to pollen fertility. *Plant Cell Rep.* **2018**, *37*, 741–757. [CrossRef] [PubMed]
62. Qiao, D.; Zhang, Y.; Xiong, X.; Li, M.; Cai, K.; Luo, H.; Zeng, B. Transcriptome analysis on responses of orchardgrass (*Dactylis glomerata* L.) leaves to a short term flooding. *Hereditas* **2020**, *157*, 20. [CrossRef] [PubMed]
63. Xu, J.; Kang, Z.; Zhu, K.; Zhao, D.; Yuan, Y.; Yang, S.; Zhen, W.; Hu, X. RBOH1-dependent H_2O_2 mediates spermine-induced antioxidant enzyme system to enhance tomato seedling tolerance to salinity-alkalinity stress. *Plant Physiol. Biochem.* **2021**, *164*, 237–246. [CrossRef] [PubMed]
64. Tran, B.Q.; Jung, S. Modulation of chloroplast components and defense responses during programmed cell death in tobacco infected with *Pseudomonas syringae*. *Biochem. Biophys. Res. Commun.* **2020**, *528*, 753–759. [CrossRef]
65. Kyu, S.Y.; Naing, A.H.; Pe, P.P.W.; Park, K.I.; Kim, C.K. Tomato seeds pretreated with Antifreeze protein type I (AFP I) promotes the germination under cold stress by regulating the genes involved in germination process. *Plant Signal. Behav.* **2019**, *14*, 1682796. [CrossRef]
66. Sandalio, L.M.; Rodriguez-Serrano, M.; Romero-Puertas, M.C.; del Rio, L.A. Role of peroxisomes as a source of reactive oxygen species (ROS) signaling molecules. *Subcell. Biochem.* **2013**, *69*, 231–255.
67. Guan, B.; Lin, Z.; Liu, D.; Li, C.; Zhou, Z.; Mei, F.; Li, J.; Deng, X. Effect of Waterlogging-Induced Autophagy on Programmed Cell Death in *Arabidopsis* Roots. *Front. Plant Sci.* **2019**, *10*, 468. [CrossRef]